AIAA JOURNAL
Vol. 39, No. 2, February 2001

Constant Voltage Anemometer Practice in Supersonic Flows

Geneviève Comte-Bellot*
Ecole Centrale de Lyon, 69131 Ecully, France
and
Garimella R. Sarma†
Tao Systems, Inc., Williamsburg, Virginia 23185

It is shown that the constant voltage anemometer (CVA) is well adapted for measurements in supersonic flows. Small hot-wire time constant, large bandwidth, high signal-to-noise ratio, variable hot-wire overheat, and independence of the cable capacitance effects of the hot wire were all observed with the CVA. Turbulence data were acquired using two methods. In the first method, signals were acquired with the CVA compensated with a fixed time constant of 0.10 ms at all test points. In situ hot-wire time constant and overheat were also acquired at each test point, which were then used in postprocessing of the turbulence signals. In the second method, full hardware compensation with the actual in situ time constant was set at each test point. The former method shows a larger bandwidth. The noise level was approximately the same in both methods. Theoretical estimates of the relative output levels of CVA, constant current anemometer, and constant temperature anemometer at different overheat ratios show that the CVA has larger output voltage level. This agrees with experimental results. CVA also had a larger bandwidth. Turbulence levels calculated using the CVA outputs agree quite well with earlier results.

Nomenclature

A, B	=	nondimensional constants in hot-wire heat loss
a_w	=	nondimensional overheating ratio, $(R_w - R_a)/R_a$
c_w	=	specific heat of hot-wire material
d	=	hot-wire diameter
E	=	mean output voltage from any anemometer
E_{CCA}	=	mean output voltage of constant current anemometer (CCA)
E_{CTA}	=	mean output voltage of constant temperature anemometer (CTA)
E_{CVA}	=	mean output voltage of constant voltage anemometer (CVA)
e'	=	fluctuating output voltage from any anemometer
e'_{CCA}	=	fluctuating output voltage of CCA
e'_{CTA}	=	fluctuating output voltage of CTA
e'_{CVA}	=	e'_{corr} for the CVA
e'_{corr}	=	software corrected output voltage of the CVA with T_C equal to M_w^{CVA}
e'_{raw}	=	fluctuating output voltage of the CVA for T_C equal to 0.10 ms
e'_u	=	uncompensated fluctuating output voltage of the CVA
F	=	power spectral density of e'
f	=	frequency
f_s	=	sampling rate
f_t	=	operational amplifier (opamp)
I_w	=	mean current in the hot-wire
i	=	digitized sample number
K	=	nondimensional CVA output defined by Eq. (18)
k_a	=	heat conductivity of air
l	=	hot-wire half-length
Ma	=	Mach number
M_w^{CCA}	=	time constant of the hot-wire operated by CCA
M_w^{CVA}	=	time constant of the hot-wire operated by CVA
m_w	=	hot-wire mass
Nu	=	Nusselt number
R	=	correlation coefficient between $(\rho u)'/\overline{\rho u}$ and $\theta'_t/\bar{\Theta}_t$
R_A	=	resistance in the CVA circuit
R_a	=	unheated hot-wire resistance
R_B, R_D, R_F	=	resistances in the CVA circuit
R_{TB}	=	top bridge resistance in the CTA circuit
R_w	=	mean heated hot-wire resistance
R_1	=	resistance in the CVA circuit
R_2	=	$R_A + R_B$
Re	=	hot-wire Reynolds number
r_L	=	lead resistance of the cable
r'	=	actual change in hot-wire resistance
r'_*	=	ideal change in hot-wire resistance
$S_{\theta_t}^{\mathrm{CCA}}$	=	sensitivity coefficient of CCA for θ'_t
$S_{\theta_t}^{\mathrm{CTA}}$	=	sensitivity coefficient of CTA for θ'_t
$S_{\theta_t}^{\mathrm{CVA}}$	=	sensitivity coefficient of CVA for θ'_t
$S_{\rho u}^{\mathrm{CCA}}$	=	sensitivity coefficient of CCA for $(\rho u)'$
$S_{\rho u}^{\mathrm{CTA}}$	=	sensitivity coefficient of CTA for $(\rho u)'$
$S_{\rho u}^{\mathrm{CVA}}$	=	sensitivity coefficient of CVA for $(\rho u)'$
s	=	Laplace operator
T	=	static temperature
T_C	=	compensation lead time constant set in the hardware circuit of the CVA
T_{θ_t}	=	turbulence intensity of θ'_t
$T_{\rho u}$	=	turbulence intensity of $(\rho u)'$
u	=	flow velocity
$\bar{u}$	=	mean flow velocity
u'	=	velocity fluctuation
u_*	=	wall friction velocity
V	=	van Driest velocity
V_w	=	voltage across the hot wire and its lead resistance
V_1	=	reference dc voltage in CVA
y	=	wall distance
α	=	temperature coefficient of resistance of hot wire
δ	=	boundary-layer thickness
$\bar{\Theta}_t$	=	mean total temperature
θ'_t	=	total temperature fluctuation
λ	=	Taylor microscale
μ	=	viscosity
ρ	=	air density
ρ_w	=	density of wire material
ρ'	=	density fluctuation
ρ_*	=	air density at wall
$(\rho u)'$	=	mass flux fluctuation

Received 15 November 1999; revision received 12 June 2000; accepted for publication 14 June 2000.

*Professor Emeritus, Mécanique des Fluides et Acoustique. Senior Member AIAA.
†Director, Research and Development.

ω_n = natural frequency of the CVA circuit
$\sim$ = frequency-domain variable
$-$ = time average

I. Introduction

THE constant voltage anemometer (CVA) and the associated circuits were patented by Sarma[1] and have been under active development since 1991. Over the years CVA prototypes were used in many applications that led to recognizing some valuable attributes of the CVA: easy operational use, high sensitivity, low time constant of the hot wire, large bandwidth, low noise, and insignificant cable capacitance effects. With the latest improvements, during the experiment or application, the CVA is operated in a free running mode, that is, data are acquired continuously without any adjustments. Necessary diagnostic voltages and waveforms were also acquired during the test that enabled the calculation of the hot-wire in situ overheat and in situ time constant for that test point. These were used to compute the turbulence in postprocessing. Sarma and Lankes[2] recently reported a fully automated version of the CVA for boundary-layer measurements in flight. The early CVA prototype using hot films has been successfully used for in-flight shock location on F-15B reported by Moes et al.[3]

The CVA practice for turbulence measurements in supersonic tunnels presented here was established with recent experiments using hot wires. However, before presenting the details, a brief review of the earlier experiments by others with CVA using hot wires will be described. The first ever systematic application of the CVA (prototype) was accomplished by Lachowicz et al.[4] and Lachowicz and Chokani[5] in hypersonic boundary-layer stability experiments. It was stated by the authors[4] that "Only the CVA, in contrast to attempts with constant current and constant temperature anemometers, provided the ability to obtain measurable signals . . . ." The reason was that the CVA was far less susceptible to electromagnetic noise than the other two anemometers in the hypersonic-tunnel environment. Through calibration in the outer boundary-layer region of the flared cone in the Mach 6 tunnel, it was observed that the hot-wire with the CVA responds to mixed mode, that is, to both mass flux and total temperature, like constant current anemometer (CCA) or constant temperature anemometer (CTA). In particular, the CVA was found to be more sensitive to mass flux at high V_w (high voltage across the hot wire, which gives high overheat) and more sensitive to total temperature at low V_w (low overheat). This feature agrees with theoretical relationships subsequently derived for the CVA by Comte-Bellot.[6] It was also observed in this calibration that the relative sensitivity (ratio of total temperature to mass flux) decreases with overheat a_w. Separately, Blanchard et al.[7] and Blanchard and Selby[8] used the same first prototype CVA to experimentally investigate the wall cooling effects on hypersonic boundary-layer stability. Because of their unique hot-wire probe design, the strain gauging of the hot wire was eliminated in those experiments. Rolloff of the spectra exhibited about 400-kHz bandwidth of that prototype in their results. Sensitivity studies were performed in these experiments with the survey of the boundary layer of the adiabatic cone at both constant V_w and constant a_w with the CVA. Trends of data sets were found to be similar in both cases, and the authors concluded that selecting more appropriate hot-wire voltage V_w would have made them equal.[8] The authors apparently were very happy with their experience with the CVA and they recommend the CVA to be the first choice anemometer for all future high-speed stability and receptivity investigations. Both these experiments used the first prototype CVA in a qualitative mode because it was felt to be sufficient, and no effort was made to investigate the quantitative approach.

A significant advance toward quantitative measurement was accomplished by Kegerise and Spina,[9] who investigated the static response features of the CVA and CTA for both subsonic and supersonic flows. Their results indicate that the relative sensitivities (ratio of total temperature to the mass flux) of the CVA and CTA follow the same quantitative trend. This trend was similar to what was obtained by Lachowicz and Chokani.[5] It was also observed by Kegerise and Spina[9] that the low overheat behavior of the CVA does not appear to be as highly nonlinear as the CTA system, thus making it particularly useful to measure gas temperature fluctuations with low overheats. Whereas Kegerise and Spina[9] have expressed the sensitivity coefficients in dimensional form, Comte-Bellot[6] derived the sensitivity coefficients in a nondimensional form. Kegerise and Spina[9] have also analyzed the Kings' law operating trajectories of the hot wire under CVA and CTA, plotting the square of the hot-wire current as a function of the flow velocity. Interesting crossings of the trajectories were observed and were explained by the authors. Sarma[10] considered the power dissipated in the hot wire, analyzed its dependence on the velocity in terms of polynomial shapes, and pointed out significant differences between CTA and CVA. In addition, Kegerise and Spina[11] did extensive studies on frequency response of CVA and CTA with laser heating of the hot wire in a jet. It was found experimentally that the frequency response of the CVA had little dependence on the operating conditions (overheat) of the wire. This interesting observation, however, was not fully understood, but was explained subsequently by Sarma.[10] The overheat change manifests as a change in the hot-wire resistance in the CVA circuit, and this change in hot-wire resistance has marginal effect on the bandwidth of the CVA circuit.

The present paper focuses on turbulence measurements in supersonic boundary layers where large bandwidths and low noise are required from the anemometer. According to Kistler,[12] the kinetic energy of the large-scale motion already encompasses eddy sizes down to one-fourth of the boundary-layer thickness, that is, 150 kHz for an external velocity of 555 m/s and a boundary-layer thickness of 15 mm. To attain structures of the order of the Taylor microscale, which is 1 mm in these conditions (see Sec. II), a bandwidth up to four times that value would be necessary. Turbulence data obtained by operating the CVA in two different methods are presented here. The first one uses a fixed compensation time constant (for the thermal inertia of the hot wire) of 0.10 ms in the CVA for all of the test points while collecting the data relating to the in situ time constant of the hot wire and its overheat. Using these in situ measured hot-wire time constant and overheat values, software processing of the CVA output signals is done for turbulence calculations. The second approach used in the present tests was to actually set the correct in situ measured time constant in the CVA hardware for proper compensation. Sarma et al.[13] earlier reported the results of CVA experiments in a Mach 2 supersonic boundary layer in the Centre d'Etudes Aérodynamiques et Thermiques (CEAT)–Poitiers facilities. In that investigation the software correction to the wire thermal lag was applied for the first time with a CVA prototype. The CVA has since been improved with even larger bandwidth, automated time constant determination, and finer hardware time constant compensation settings. The improved CVA was used for boundary-layer measurements at the Marseille/Institut de Recherche sur les Phénomènes Hors Equilibre (IRPHE) supersonic wind tunnel. This wind tunnel has several important features useful for the CVA study. It is a continuous tunnel with very steady flow within $\pm 1\%$ allowing accurate data recording. The stagnation pressure is adjustable from 0.12 to 0.80×10^5 Pa, hence permitting the time constant M_w^{CVA} of the hot wire under the constant voltage operation to be analyzed at various Reynolds numbers. A basic zero pressure gradient turbulent boundary layer at Mach 2.3 is also available, so that the CVA output can be analyzed within a well-documented context. The IRPHE group also has CCA and CTA systems along with vast experience contributing to valuable comparisons with the CVA.

II. Experiments

Wind Tunnel

Three pressures were used in the IRPHE wind tunnel: 0.163, 0.492, and 0.746×10^5 Pa. The nominal stagnation temperature was 285 K, with Mach number fixed at 2.3, giving a freestream velocity of 555 m/s and a static temperature of 145 K. The mean aerodynamic characteristics of the boundary layer developed on the floor of the test section have already been well documented. At a downstream distance of 0.75 m from the sonic throat, the boundary-layer thickness δ was 15 mm and the wall friction velocity $u_* = 22$ m/s. At the wall distance chosen for the turbulence experiments, $y = 4.1$ mm, that is, $y/\delta = 0.27$, the Mach number was 1.612, with a velocity 451.1 m/s, and the static temperature 194.8 K. At that distance, for the intermediate pressure of 0.492×10^5 Pa, the

air density was $\rho = 0.071$ kg/m^3 and the air density at the wall was $\rho_* = 0.0485$ kg/m^3.

Hot Wire

The hot wire was tungsten with a diameter $d = 2.5$ μm with a length $2l = 0.5$ mm giving an aspect ratio of 200. This aspect ratio is similar to those currently used, which are in the range 160–300, as listed in Table 1 of Dussauge et al.[14] Many parameters affect the end loss in hot wires: wire material, nature of the wire junction to the broaches (in supersonic flows epoxy is often added to avoid vibrations), ability of the supports to stay in equilibrium with the mean ambient temperature, nature of the incident fluid, wire Reynolds number, slack introduced in the wire so as to avoid strain-gauge peaks, and the asymmetries in the wire temperature distribution. Analysis of the end effect in an academic case, most often a subsonic flow, however, can be used as a qualitative guide for the supersonic case. Estimates by Corrsin[15] for the CCA and by Ko et al.[16] and Fingerson and Freymuth[17] for the CTA are available in literature. Generally an estimated 20% thermal end loss is often found. However, the sensitivity coefficients with which the turbulence calculations are done are not very much affected by the end losses. In Ref. 16, it is shown that the end loss does not change with overheat above 0.20 for different Reynolds number. The numerous experimental calibration tests done by Morkovin,[18] Gaviglio,[19] Bonnet,[20] and Smits et al.,[21] among others, also show the same trend. For example, the relative sensitivity coefficient $S_{\theta_t}^{\mathrm{CCA}}$ to recovery temperature in CCA varies from 1.1 to 0.90 when overheat increases from 0 to 0.50, compared to a theoretical value of 1.00; the relative sensitivity $S_{\rho u}^{\mathrm{CTA}}$ to mass flux fluctuations in CTA stays in the narrow range 0.23–0.24, very close to the theoretical value of 0.25. Moreover, as indicated by Fingerson and Freymuth,[17] the mass flux fluctuations are less affected than the temperature fluctuations due to end loss. This feature is very useful for supersonic boundary layers, where the mass flux fluctuations are dominant.

As to the spatial resolution permitted by the wire, the wire length was about half the transverse Taylor microscale λ, of the flow. This estimate was made using the relation

$$\lambda^2 = 15\frac{\mu}{\rho}\frac{\overline{u'^2}}{|\overline{u'v'}|}\frac{1}{\mathrm{d}\bar{u}/\mathrm{d}y}$$

which expresses a balance between turbulence production and dissipation. The viscosity μ is given by $\mu = 17.1 \times 10^{-6}(T/273)^{0.75}$, the relative Reynolds stress $|\overline{u'v'}|/\overline{u'^2}$ approaches 0.30, and the mean velocity gradient $\mathrm{d}\bar{u}/\mathrm{d}y$ deduced from the logarithmic law that applies to the van Driest velocity

$$V = \int_0^{\bar{u}} \left(\frac{\rho}{\rho_*}\right)^{\frac{1}{2}} \mathrm{d}\bar{u},$$

so that $\mathrm{d}V/\mathrm{d}y = u_*/ky$ (where k is the von Kármán constant) and $\mathrm{d}\bar{u}/\mathrm{d}y = (\rho_*/\rho)^{1/2}(\mathrm{d}V/\mathrm{d}y)$. This ensemble gives $\lambda \approx 1$ mm at $y = 4.1$ mm. The error on the turbulence rms value, therefore, is small, around 4%, using the classic relation[6] $\overline{u'^2_{\mathrm{meas}}} = \overline{u'^2_{\mathrm{exact}}}[1 - \frac{1}{6}(2l/\lambda)^2]$. The wire Reynolds numbers, $Re = \rho\bar{u}\,\mathrm{d}/\mu_t$ with the viscosity estimated at stagnation temperature, were 2.5, 7.4, and 11.2 in the external flow at pressures of 0.163, 0.492, and 0.746×10^5 Pa, respectively. The hot-wire time constant values were measured at these Reynolds numbers under different CVA test conditions. $Re = 6.0$ in the boundary layer at a wall distance $y = 4.1$ mm, where the turbulence was measured, for a pressure of 0.492×10^5 Pa. The hot-wire time constant was also measured at this point under different CVA test conditions.

CVA System

Figure 1 is a schematic of the CVA system. A detailed transfer function was presented by Sarma.[10] Any change in wire resistance due to fluid flow produces a current change in the hot wire, the path for which is only through the large resistor $R_2 = (R_A + R_B)$ of the circuit. The output signals, E_{CVA} and e'_{CVA}, for the mean and fluctuating parts will, therefore, be large. They can be directly recorded without any further amplification. The voltage V_w across the wire is fixed by the resistances R_F, R_1, and the dc voltage V_1 of the reference source, and it can be finely and continuously adjusted from 0.005 to 2 V. The dc operating relations established by Sarma[10] for the basic system are given by

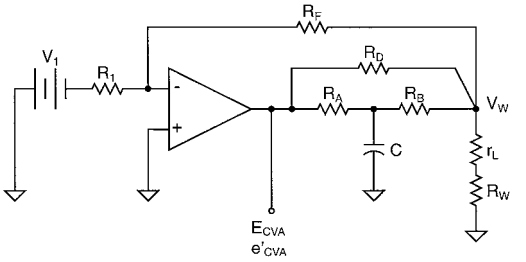

Fig. 1 Basic CVA circuit with hot-wire thermal lag compensation.

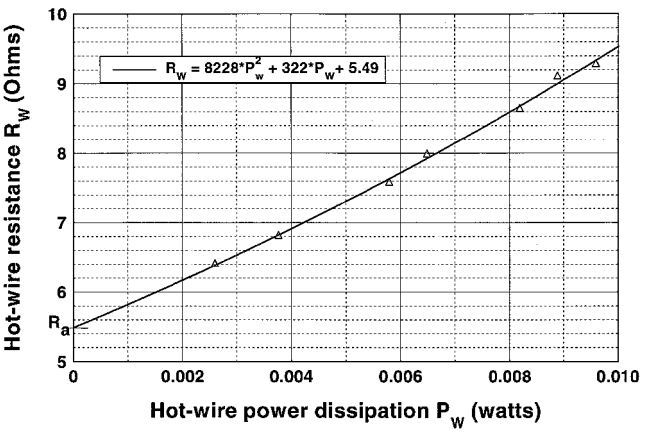

Fig. 2 Estimating the in situ cold resistance R_a from measured power dissipation.

$$V_w = (R_F/R_1)V_1 \tag{1a}$$

$$E_{\mathrm{CVA}} = V_w + R_2 V_w[1/(R_w + r_L) + 1/R_F] \tag{1b}$$

$$R_w + r_L = R_2/[E_{\mathrm{CVA}}/V_W - (1 + R_2/R_F)] \tag{1c}$$

V_w represented by Eq. (1a) is independent of all other resistances in the feedback in the normal linear operation of the operational amplifier. Equation (1c) is used to estimate the wire resistance R_w from the in situ measured E_{CVA} and V_w values. In practice, the actual values of R_2 ($\approx$100 Ω) and $1 + R_2/R_F$ ($\approx$1.3) are obtained by calibration of the CVA with precision resistors. Such a calibration takes into account all of the component tolerances and circuit wiring.

The cold resistance of the hot wire R_a in every case was estimated from the plot of the measured hot-wire resistance R_w, with the electric power injected into the wire at different overheats and extrapolating the curve toward zero power dissipation for the cold resistance value. Such a plot for the present experiments is shown in Fig. 2. The R_a value estimated with the CVA agrees within ± 1% of that estimated independently with CCA. The wire recovery factor is taken equal to 1, for simplicity, although its exact value would be 0.95 for the Reynolds number values[19] of the test. The same hot wire was kept for all of the measurements, including the comparisons with CCA and CTA. Its cold resistance was $R_a = 5.50$ Ω. The cable resistance was 0.64 Ω for a 4-m-long Dantec cable, and the lead resistance of the hot-wire probe was 0.50 Ω, thus giving a total cable lead resistance $r_L = 1.14$ Ω. This value is taken into account in all data processing.

Measurement of the wire time constant M_w^{CVA} is made in situ by injection of a 20-Hz square wave at the junction of R_1 and R_F. A detailed description of the method was presented by Sarma.[10] A T_C range from 0.10 to 0.50 ms is covered in 0.01-ms steps in the present CVA prototype for hardware compensation purposes.

Spectral Plots

All of the turbulence signals were acquired with 1-MHz sampling rate with a LeCroy 8007, module 8901A. For the time constant

tests, the sampling frequency was 100 kHz. For the CVA, at each data point, 127 blocks of 4096 samples per block were acquired for averaging. In addition to the usual power spectral density (PSD) of signals, denoted $F(f)$, where f is frequency, the frequency-weighted PSD, $fF(f)$ has also been used:

$$\overline{e'^2} = \int_0^\infty F(f)\,\mathrm{d}f = \int_0^\infty fF(f)\frac{\mathrm{d}f}{f} = \int_0^\infty fF(f)\,\mathrm{d}\ln f \quad (2)$$

The plot between $fF(f)$ on the y axis and $\ln f$ on the x axis will be linear. In all of the PSD plots in this paper, $\ln f/2.3$ is shown as an additional x axis in the upper scale because it permits direct correspondence with frequency f. By simple visual inspection of the highest part of $fF(f)$ or the plateau, the frequency range that contributes to the most of the mean square output voltage can be recognized. Note that wall turbulence spectra will have a large region with an f^{-1} slope for wall distances belonging to the logarithmic zone, as described by Dussauge et al.[14] Present measurements at $y = 4.1$ mm, that is, $y/\delta = 0.27$, are close to that zone so that a plateau in the turbulence spectra of $fF(f)$ can be expected.

III. Hot-Wire Time Constants with CVA

The measured time constants M_w^{CVA} of the hot-wire under the CVA operation are shown in Fig. 3 along with the associated time constants M_w^{CCA} of the same wire operated with the CCA. The change in hot-wire resistance can be represented by the simple first-order differential equation:

$$r' + M\frac{\mathrm{d}r'}{\mathrm{d}t} = r'_* \quad (3)$$

where r' is the actual response of the hot wire and r'_* is the ideal response of the hot wire that would be in perfect equilibrium with the flow. $M = M_w^{\mathrm{CVA}}$ with CVA, and $M = M_w^{\mathrm{CCA}}$ with CCA. From Figs. 3 and 4, the following observations can be made. M_w^{CVA} decreases significantly with the overheat a_w, and it is always less than M_w^{CCA} under the same operating conditions. The reduction in time constant under the CVA operation was predicted independently by Freymuth,[22] Sarma,[10] and Comte-Bellot.[6] It can be represented by

$$M_w^{\mathrm{CVA}} = M_w^{\mathrm{CCA}}\Big/(1 + 2a_w) \quad (4)$$

Measured values thus are very close to Eq. (4). As a consequence, the reduced time constant in CVA operation requires lower compensating gain in the CVA for a given bandwidth compared to CCA, which in turn contributes to lower noise levels in CVA. Measured time constants at $Re = 6$ and 7.4 indicate that the in situ time constants are accurate even in the presence of turbulence because of averaging. Figure 4 shows that the time constant of the hot wire M_w^{CVA} under the constant voltage operation decreases with the wire Reynolds number Re. Recent measurements by Sarma and

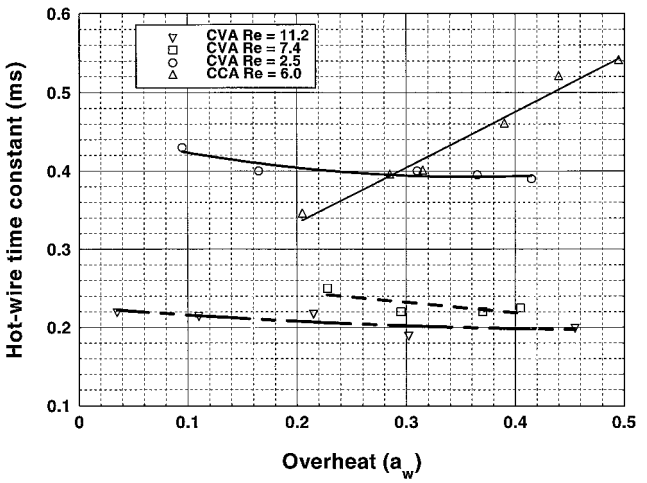

Fig. 3 Hot-wire time constants at different Reynolds numbers Re and overheats a_w for CVA and CCA (tungsten wire $d = 2.5$ μm, and $2l = 0.5$ mm).

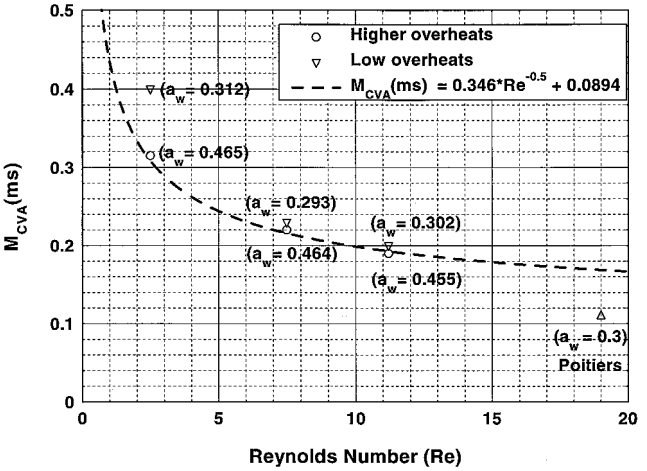

Fig. 4 Time constant variation of the hot-wire with CVA as a function of Reynolds number.

Lankes[2] in subsonic flows have clearly established that trend, which also exists with a CCA in supersonic conditions, as indicated in the pioneering work of Kovasznay.[23] To quantify this feature, the classic expression of the hot-wire time constant[6] should be examined:

$$M_w \equiv M_w^{\mathrm{CCA}} = (R_w - R_a)(m_w c_w/R_a\alpha)\left(1\Big/R_a I_w^2\right) \quad (5)$$

Using the Collis–Williams/Kovasznay law, $Nu = A + B\sqrt{(Re)}$, Eq. (5) becomes

$$M_w^{\mathrm{CVA}} = \frac{1 + a_w}{1 + 2a_w}\frac{d^2}{4}\frac{\rho_w c_w}{k_a}\frac{1}{A + B\sqrt{Re}} \quad (6)$$

Constant B is always in the narrow range 0.56–0.58, but the constant A varies considerably. According to the extensive analysis made by Dewey,[24] $A = 0.24$ in subsonic and relatively high Reynolds numbers $Re \approx 10$–100, $A = -0.79$ for high supersonic $Ma > 2$ with very high Reynolds numbers $Re \approx 50$–200, and $A \approx 0$ for $Ma > 2$ and Re in the range 2–11. Present experiments used low pressures with $Ma > 2$; therefore, we can assume $A \approx 0$. With $A = 0$, M_w^{CVA} will follow Reynolds number $Re^{-1/2}$ law [Eq. (6)], and this trend is very distinctly seen in Fig. 4. Kuppa et al.[25] indicated that aspect ratio does not play a significant role on the time constant under the constant voltage operation. In Fig. 4, the single smaller M_w^{CVA} value of 0.11 ms obtained in the supersonic facilities at the University of Poitiers, reported by Sarma et al.,[13] corresponds to $d = 2.5$ μm, $2l = 0.5$ mm, $a_w = 0.80$, $Ma = 2.0$, and $Re = 19$. This smaller value in time constant is attributed to the smaller Knudsen number $Kn \approx Ma/Re$.

IV. Thermal Lag Compensation and Bandwidths

The thermal lag compensation has to restore r'_* from the measured r'. Figure 5 shows the required gain for such a restoration as a function of frequency. A gain ceiling value of 1000 has been selected corresponding to the commercial CCA used at IRPHE, and it also covers reasonably well the CVA prototype. The advantage of having a smaller time constant T_C for compensation is clear because it permits large bandwidth to be obtained. The transfer function of the CVA can be represented by[10]

$$\frac{\tilde{e}'_{\mathrm{CVA}}}{\tilde{u}'}(s) = \left[\frac{(R_2/R_w)I_w}{s^2\Big/\omega_n^2 + \left[(1/T_C + (R_w/R_d)2\pi f_t)\Big/\omega_n^2\right]s + 1}\right] \times \left[\frac{(1 + T_C s)}{\left(1 + M_w^{\mathrm{CVA}} s\right)}\right] b' \quad (7)$$

Equation (7) relates the perturbation output voltage $\tilde{e}'_{\mathrm{CVA}}$ to velocity fluctuation $\tilde{u}'$ in the frequency domain. The loss in sensitivity of the hot wire due to M_w^{CVA} manifests as a pole, which is compensated by the CVA with a zero with the hardware resistance–capacitance

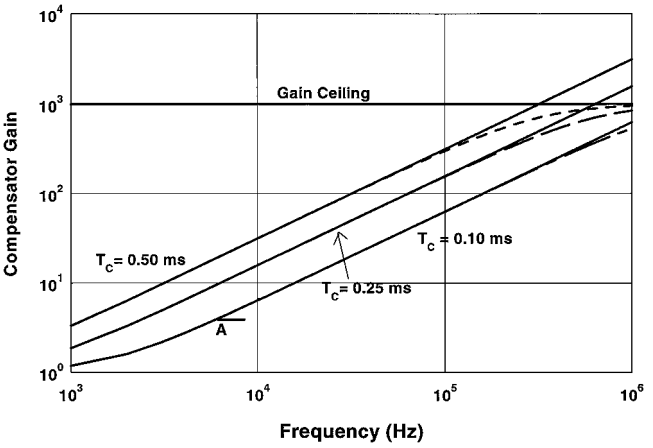

Fig. 5 Compensator gains at different compensation settings T_C.

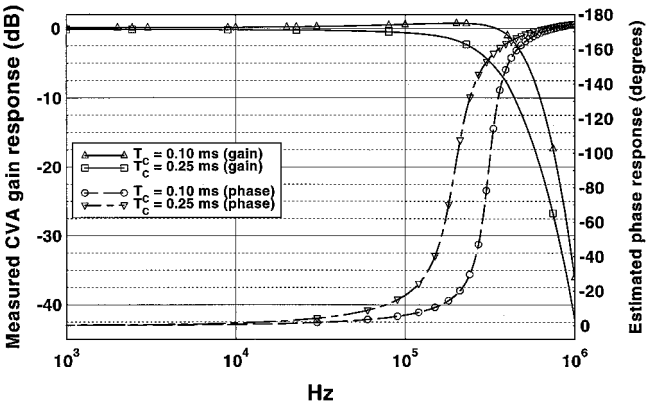

Fig. 6 Measured frequency response and estimated phase response of the CVA at two compensator time constants, T_C.

(RC) combination (Fig. 1) time constant T_C. With proper compensation $T_C = M_w^{\mathrm{CVA}}$, the frequency response will be limited by only the amplifier terms in the first bracket.

Compensation Methods

In the present boundary-layer measurements, two compensation methods were used. The first method applied only a partial compensation in hardware with a lower time constant ($T_C = 0.10$ ms) than the in situ measured M_w^{CVA} value ($M_w^{\mathrm{CVA}} \cong 0.25$ ms), and necessary corrections were applied to the acquired data with software in postprocessing. This method is highly productive because it does not require any adjustment during the test. In the second method, CVA hardware compensation T_C was set to be equal to that of the in situ measured hot-wire time constant M_w^{CVA}, that is, $T_C = M_w^{\mathrm{CVA}}$ in Eq. (7), giving a full hardware compensation in the CVA itself. First method gives larger bandwidth than the second full hardware compensation method. The CVA prototype tested had 470 and 270 kHz bandwidths, respectively, at 0.1 and 0.25 ms T_C settings, as shown in Fig. 6. The procedure to determine the bandwidth was given by Sarma.[10] The software processing used in the second method described retains the larger bandwidth associated with the smaller T_C setting.

Software Processing and Its Validity

For proper operation of the CVA, T_C should be set equal to the actual M_w^{CVA} value thereby canceling the expression in the second bracket in Eq. (7). This reduces the response of the CVA to a simple second-order system. In the software processing method, the data from CVA were collected by using a fixed compensation setting ($T_C = 0.10$ ms) while also collecting the in situ M_w^{CVA} data at each test point, without actually matching them during the test. In postprocessing, the M_w^{CVA} value is computed from the acquired time constant data. To apply the correction, the CVA output was modified by the following equation in the frequency domain:

$$\tilde{e}'_{\mathrm{corr}} = \tilde{e}'_{\mathrm{raw}} \left[\frac{1 + M_w^{\mathrm{CVA}} s}{1 + T_C s} \right] \tag{8}$$

which gives in the time domain

$$e'_{\mathrm{corr}} + T_C \frac{\mathrm{d}e'_{\mathrm{corr}}}{\mathrm{d}t} = e'_{\mathrm{raw}} + M_w^{\mathrm{CVA}} \frac{\mathrm{d}e'_{\mathrm{raw}}}{\mathrm{d}t} \tag{9}$$

A partial lead compensation in the CVA with T_C gives the CVA output as

$$e'_{\mathrm{raw}} = e'_u + T_C \frac{\mathrm{d}e'_u}{\mathrm{d}t} \tag{10}$$

where e'_u is the uncompensated output of the CVA, and a full lead compensation in the CVA would give

$$e'_{\mathrm{corr}} = e'_u + M_w^{\mathrm{CVA}} \frac{\mathrm{d}e'_u}{\mathrm{d}t} \tag{11}$$

Taking the Laplace transform of Eqs. (10) and (11) and taking their ratio eliminates the uncompensated e'_u and gives Eq. (8). Equation (9) can now be written as a difference equation,

$$T_C \frac{\Delta e'_{\mathrm{corr}}}{\Delta t} = (e'_{\mathrm{raw}} - e'_{\mathrm{corr}}) + M_w^{\mathrm{CVA}} \frac{\Delta e'_{\mathrm{raw}}}{\Delta t} \tag{12}$$

or in terms of the ith and $(i-1)$th samples of voltages with a sampling rate $f_s = 1/\Delta t$,

$$e'_{\mathrm{corr}}(i) = \left\{ e'_{\mathrm{raw}}(i) + f_s \left\lfloor M_w^{\mathrm{CVA}} [e'_{\mathrm{raw}}(i) - e'_{\mathrm{raw}}(i-1)] + T_C e'_{\mathrm{corr}}(i-1) \right\rfloor \right\} \Big/ (1 + T_C f_s) \tag{13}$$

where any initial condition can be used. As the frequency increases, Eq. (8) or Eq. (9) shows that the following asymptotic value is approached:

$$e'_{\mathrm{corr}}(t) = \left(M_w^{\mathrm{CVA}} \Big/ T_C \right) e'_{\mathrm{raw}}(t) \tag{14}$$

Equation (14) relates the rms values well above a certain frequency, depending on the numerical values of the time constants. The frequency above which Eq. (14) will be valid is identified as point A in Fig. 5, from where the rise is linear with frequency and, hence, is above around 6 kHz for $T_C = 0.10$ ms. The validity of the correction represented by Eq. (13) was investigated at different frequencies with sine wave input signal $\sin 2\pi f t$ by comparing the software corrected signal to the input. It was found that irrespective of the time constants, the software correction was accurate up to half the sampling frequency. As an example, a typical 100-kHz input signal and the corresponding corrected output are shown in Fig. 7a. In addition, Fig. 7b for 10 kHz shows the high fidelity of the asymptotic corrected output [Eq. (14)] comparing it to the software corrected output using Eq. (13). In the present investigation, software processing was, however, applied using the full correction represented by Eq. (13), not the asymptotic relationship. Thus, this new approach corrects the data in postprocessing with in situ measured M_w^{CVA} value while setting a smaller T_C (larger bandwidth) in the CVA hardware. This approach is possible with the CVA because its transfer function is well defined and is independent of any first-order effects of hot-wire cable capacitance, unlike the other anemometers.

V. Noise Measurements

The CVA noise was measured by keeping the hot wire in the wind tunnel, but with no airflow, so that all of the wire connections were kept unchanged. PSD plots, with the associated rms values of the typical noise, are shown in Fig. 8. Several conclusions can be drawn from these plots. The spikes in noise spectra are relatively small in CVA compared to the other anemometers. This feature was observed early, even with the first prototype CVA in the hypersonic wind-tunnel tests at NASA Langley Research Center.[4] The PSD is almost flat for $T_C = 0.10$ ms. There is just a slight f^{+1} increase associated due to the increased compensator gain with frequency. At $T_C = 0.25$ ms, the increase is more pronounced, as expected. The spurious noise increase as f^{+2} was not observed in CVA in the present experiments, unlike the CTA, which showed such a noise

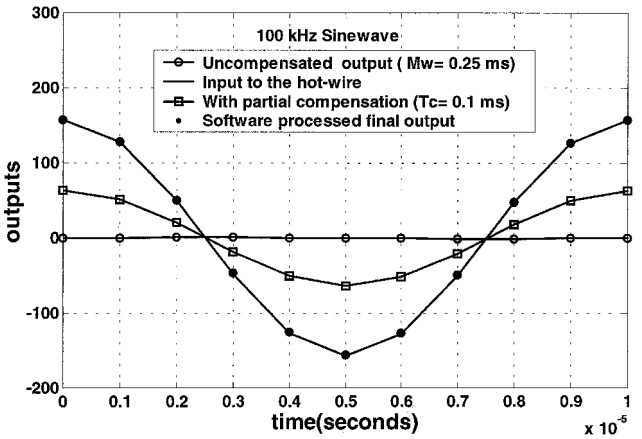

Fig. 7a Validity of software correction at 100 kHz.

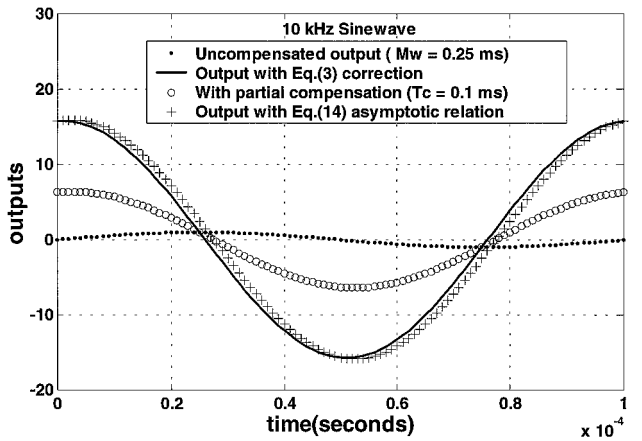

Fig. 7b Validity of the asymptotic compensation relationship Eq. (14) at $f = 10$ kHz.

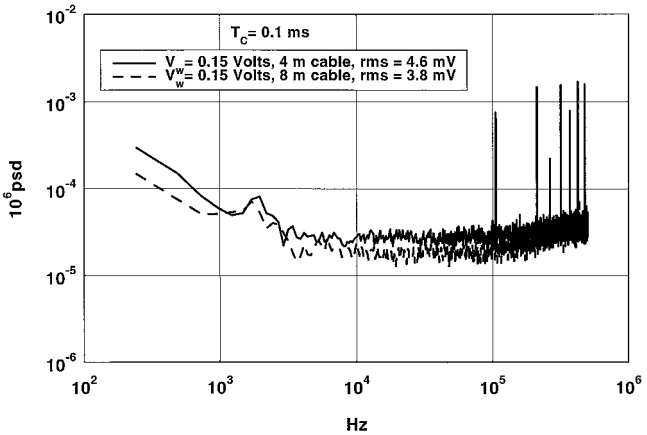

Fig. 8 CVA noise spectra at $T_C = 0.10$ ms for two cable lengths.

spectra with four different CTA products, as reported by Saddoughi and Veeravalli.[26] Fingerson and Freymuth[17] also predicted such a behavior for the CTA noise. The smaller noise level observed with the 8-m cable compared to the 4-m cable is an effect of the sensitivity loss due to increased lead resistance from the cable. Increased cable capacitance associated with the 8-m cable did not change the spectra. Only slight increase in rms with increased T_C in CVA was observed.

VI. Full Hardware-Compensated CVA Spectra

Turbulence spectra obtained at $y = 4.1$ mm when the CVA hardware compensation time constant T_C was set equal to the in situ measured hot-wire time constant $M_w^{\mathrm{CVA}} = 0.25$ ms for proper compensation is shown in Fig. 9. The measured bandwidth of the CVA at this point was 270 kHz. The rms values of the turbulence signals were 61 and 40 mV for 0.64 and 0.17 overheats, respectively. The noise spectra with this setup, with a voltage across the hot wire at $V_w = 0.15$ V and a 4-m-long cable, is also shown. Only the frequency-weighted representation $fF(f)$ of the spectra was used to point out the most energetic frequencies, as explained in Sec. II. The flat region in the $fF(f)$ plot also shows the extent of the f^{-1} region of the turbulence energy in the boundary layer. It can be seen in Fig. 9 that there is a flat plateau up to just over 100 kHz, particularly with the higher overheat. Signal-to-noise ratio from the PSD is about 25 dB at 100 kHz, 16 dB at 200 kHz, and 0 dB at 400 kHz. Distinct strain gauge peaks are visible in the spectra around 170 and 350 kHz. Such strain gauging peaks are possible from hot wires in supersonic flows.[14]

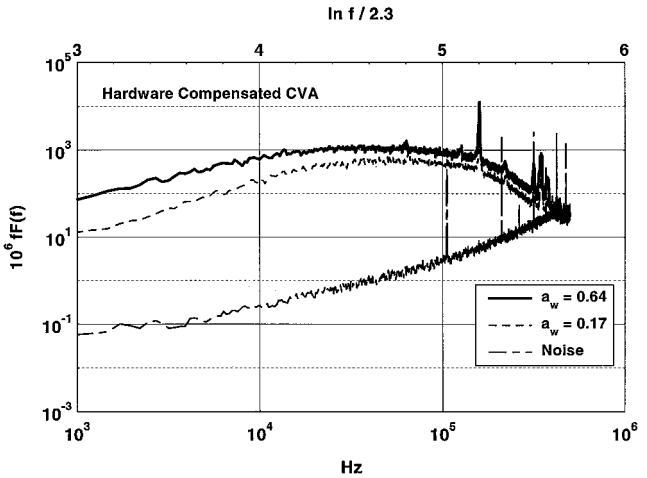

Fig. 9 Full hardware in situ compensated CVA response at two overheats with noise in the $fF(f)$ vs $\ln f$ representation.

VII. Raw and Software-Processed CVA Spectra

The data collected with the CVA compensation set at $T_C = 0.10$ ms are referred to as raw data. They are shown again at the same two overheats used in hardware compensation (0.17 and 0.64) in Fig. 10 in the frequency-weighted spectra form. Also shown is the noise spectrum corresponding to $T_C = 0.10$ ms, $V_w = 0.15$ V, and a 4-m-long cable. These raw data are the original signals from the CVA at the selected fixed hardware time constant T_C. These signals have significance in that they permit the assessment of the quality of the original signals from the CVA before any transformation with software. The rms values of the raw signals were 16.7 and 27 mV for 0.17 and 0.64 overheats, respectively. Examination of the spectra shows that the noise level remained the same as the full hardware-compensated case. The turbulence signal levels were smaller due to inadequate compensation. However, the signal-to-noise ratio becomes unity (0 dB) at 500 kHz in this case, instead of 400 kHz as noted in the hardware-compensation case. The plateau of the spectra, although lower (due to partial compensation with a smaller time constant than the actual hot-wire time constant), shows an extended region when compared to the hardware compensation. This is because of larger bandwidth of the CVA with a smaller time constant setting.

The software compensation explained in Sec. IV is now applied to the raw data and the noise with the appropriate M_w^{CVA} value in each case. The results are presented in Fig. 11. The compensation algorithm was also applied to the raw noise data at $T_C = 0.10$ ms, and the resultant spectra are also shown in Fig. 11. This noise representation may not be the exact behavior but, nevertheless, represents the worst-case representation. Several distinct features can be noted from the software-processed spectra shown in Fig. 11. Even after the software correction, the signal-to-noise ratio was at the same level as in the raw data case. The plateau height is the same for the software-compensated spectra and for the full hardware-compensated spectra. The frequency extent of the plateau is notably larger in software-compensated spectra than the hardware compensation. It goes up

Table 1 Operating conditions of the CVA tests

V_w, V	E, V	Overheat a_w	Time constant M_w^{CVA}, ms	e' (rms), mV: Raw signals	Software-processed output	Hardware-compensated output
0.152	2.20	0.169	0.299	16.7	53.8	40.0
0.187	2.58	0.243	0.300	20.6	61.8	——
0.241	3.06	0.383	0.266	23.1	61.6	——
0.260	3.17	0.457	0.252	24.9	62.9	——
0.319	3.55	0.637	0.248	27.0	67.9	61.0
0.335	3.63	0.694	0.250	28.3	70.8	——

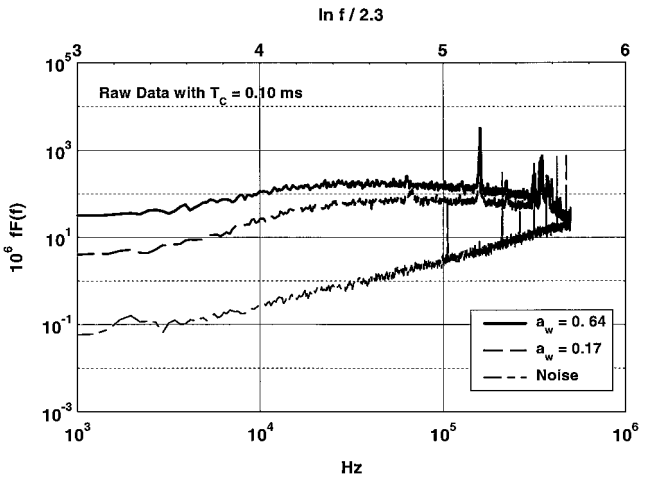

Fig. 10 Raw CVA data at two overheats with noise in the $fF(f)$ vs $\ln f$ representation.

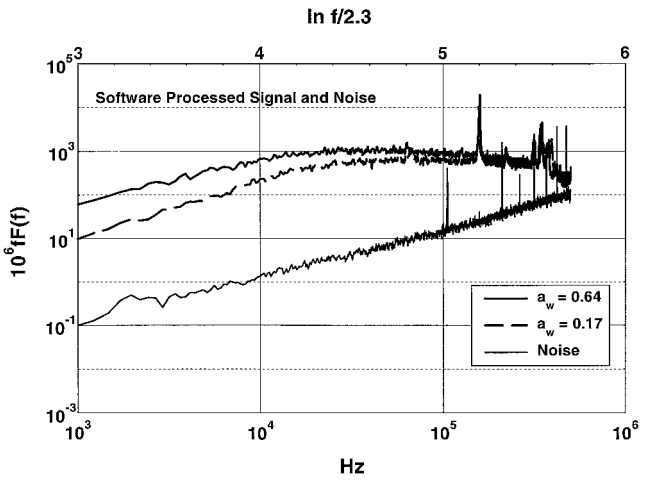

Fig. 11 Software-processed CVA response at two overheats with the estimated noise using the same correction in the $fF(f)$ vs $\ln f$ representation.

to about 300 kHz, compared to only 100 kHz in the hardware-compensated method. This is a clear illustration of the larger bandwidth offered by the software procedure. The asymptotic relationship given by Eq. (14), $e'_{corr} = (M_w^{CVA}/T_C)e'_{raw}$ between the raw and software-processed rms values is also well validated. Tables 1 and 2 list all of the data for the turbulence measurements. The tables give a summary of the operating conditions and outputs of the CVA, CTA, and CCA in IRPHE Mach 2.3 boundary layer, pressure $= 0.492 \times 10^5$ Pa, $y/\delta = 0.27$ with tungsten hot wire $d = 2.5$ μm and $2l = 0.5$ mm. The hardware-corrected rms values are 40 mV at $a_w = 0.17$ and 61 mV at $a_w = 0.64$, whereas the software-corrected values at the same overheat are 54 and 68 mV, respectively. Smaller rms values from the hardware compensation are because of its smaller bandwidth.

Table 2 Operating conditions of CCA and CTA tests

I_w (hot-wire current), mA	E, V	Overheat a_w	Time constant M_w^{CCA}, ms	e' (rms), mV
		CCA		
21	0.1506	0.17	0.320	4.35
30	0.2686	0.50	0.545	11.9
		CTA		
——	0.865[a]	0.60	——	26.8

[a]Top of the bridge.

VIII. Turbulence Estimates Using the CVA Data

CVA Output Relationship to Turbulence

Mass flux fluctuations $(\rho u)'$ and total temperature fluctuations θ'_t are the only predominant perturbations with the Mach number 2.3 used in the present study. Therefore, the following intensities and correlation coefficients are required:

$$\frac{\overline{(\rho u)'^2}}{(\overline{\rho u})^2} = T_{\rho u}^2, \qquad \frac{\overline{\theta_t'^2}}{\bar{\Theta}_t^2} = T_{\theta_t}^2, \qquad \frac{\overline{(\rho u)'\theta_t'}}{\overline{\rho u}\bar{\Theta}_t} = R \tag{15}$$

(with $\overline{\rho u} \approx \bar{\rho}\bar{u}$). Quantitative measurements with the CVA are made possible with simple sensitivity relationships derived by Comte-Bellot[6] and extensive calibration data obtained using CCA and CTA as reported in Sec. II. More precisely, the relative CVA output is

$$e'_{CVA}/E_{CVA} = S_{\rho u}^{CVA}[(\rho u)'/\overline{(\rho u)}] + S_{\theta_t}^{CVA}(\theta_t'/\bar{\Theta}_t) \tag{16}$$

with the relative sensitivity coefficients given by

$$S_{\rho u}^{CVA} = \frac{S_{\rho u}^{CTA}}{1+2a_w} \approx \frac{1}{4(1+2a_w)}$$

$$S_{\theta_t}^{CVA} = \frac{S_{\theta_t}^{CCA}}{1+2a_w} \approx \frac{1}{(1+2a_w)} \tag{17}$$

Taking the mean square of Eq. (16) gives, after some rearrangements,

$$K \equiv \left[\frac{\overline{e'^2_{CVA}}}{E^2_{CVA}}(1+2a_w)^2\right] = \left[\frac{a_w^2}{4}T_{\rho u}^2 - a_w R + T_{\theta_t}^2\right] \tag{18}$$

All of the quantities in the first bracket are measured during the test at each overheat setting. On the plot of K vs a_w (Fig. 12), the value of K for $a_w = 0$ gives $T_{\theta_t}^2$; the presence of a minimum in the plot indicates that $R > 0$ and, conversely, the absence of a minimum indicates that $R < 0$. Data should be acquired for at least three overheats a_w but data with more overheat settings permit reduction of the experimental scatter. With the new CVA prototype, the overheat can be easily changed remotely without holding up the experiment. For the present data shown in Tables 1 and 2, using the software-processed rms values, a polynomial fit corresponding to the second bracket in Eq. (18) was then obtained, as shown in Fig. 12. The coefficients of the polynomial give the following turbulence quantities:

$$\frac{\sqrt{\overline{(\rho u)'^2}}}{\overline{\rho u}} = 13.5\%, \qquad \frac{\sqrt{\overline{\theta_t'^2}}}{\bar{\Theta}_t} = 3.5\%$$

$$\frac{\overline{(\rho u)'\theta_t'}}{\sqrt{\overline{(\rho u)'^2}}\sqrt{\overline{\theta_t'^2}}} = 0.30 \tag{19}$$

All of the computations also take into account the cable resistance r_L, which divides R_w by a factor $(1 + r_L/R_w)$ in all of the sensitivity coefficients.

Estimation of Nondimensional Turbulence Intensity

Finally, the procedure for the estimation of turbulence intensity (from CVA test results) in the nondimensional form $\sqrt{(\bar{\rho}\overline{u'^2}/\rho_* u_*^2)}$, which takes into account the $\sqrt{(\bar{\rho}/\rho_*)}$ transformation as in mean velocity profiles, is presented. The two usual main assumptions[14]

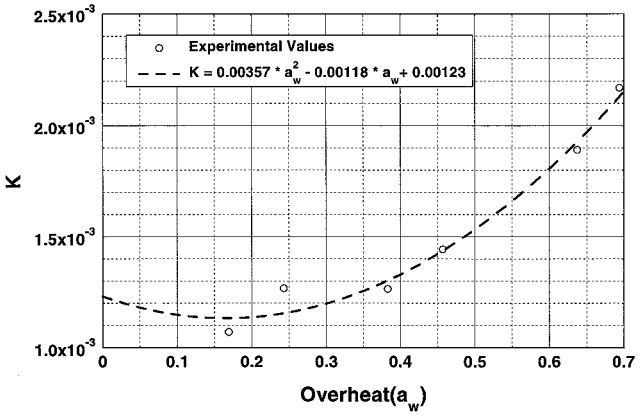

Fig. 12 Plot of $K = (\overline{e'^2_{\mathrm{CVA}}}/E^2_{\mathrm{CVA}})(1+2a_w)^2$ vs overheat with its polynomial fit to estimate the turbulence intensities and correlation coefficient.

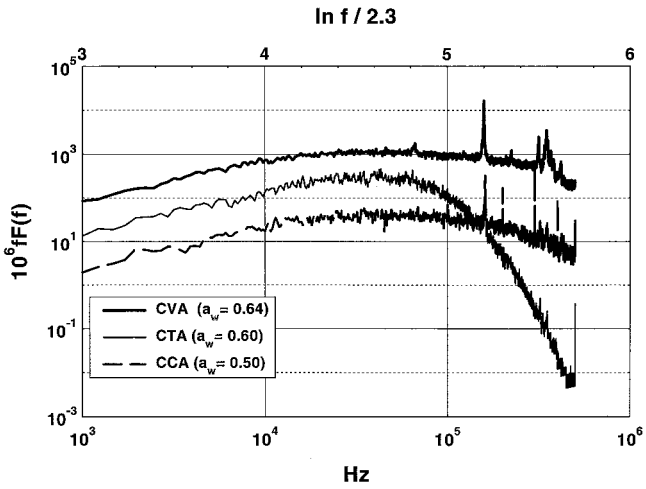

Fig. 13 Comparison of CCA, CTA, and software-corrected CVA responses at high overheat in the $fF(f)$ vs $\ell n f$ representation.

are valid: The static pressure and stagnation temperature across the boundary layer are constant and the strong Reynolds analogy (SRA) is also valid. The relative mass flow change $(\rho u)'/\bar{\rho}\bar{u}$ is first transformed into

$$(\rho u)'/\bar{\rho}\bar{u} = [(\bar{\rho}+\rho')(\bar{u}+u') - \bar{\rho}\bar{u}]/\bar{\rho}\bar{u} \approx \rho'/\bar{\rho} + u'/\bar{u} \qquad (20)$$

neglecting higher-order terms in fluctuations. The assumption of constant stagnation temperature and constant static pressure permits relating the rms value of ρ' to that of u' by

$$\sqrt{\overline{\rho'^2}}\big/\bar{\rho} \approx (\gamma-1)Ma^2\left(\sqrt{\overline{u'^2}}\big/\bar{u}\right) \qquad \text{with} \qquad \gamma = 1.4 \qquad (21)$$

The SRA provides the following correlation coefficient between ρ' and u':

$$\overline{\rho' u'} \approx 0.80\sqrt{\overline{\rho'^2}}\sqrt{\overline{u'^2}} \qquad (22)$$

Hence,

$$\overline{(\rho u)'^2}/\bar{\rho}^2\bar{u}^2 \equiv T^2_{\rho u} = (\overline{u'^2}/\bar{u}^2)[(\gamma-1)^2Ma^4 + 1.6(\gamma-1)Ma^2 + 1] \qquad (23)$$

Equation (22) can now be solved for $\overline{u'^2}/\bar{u}^2$ because $T^2_{\rho u}$ is known from experiments. Using the value from Eq. (19) $T_{\rho u} = 13.5\%$ and the aerodynamic parameters $\bar{\rho}$, $\bar{u}$, Ma, ρ_*, and u_* listed in Sec. II for $y/\delta = 0.27$ gives

$$\sqrt{\bar{\rho}\overline{u'^2}}\big/\rho_* u_*^2 \approx 1.75 \qquad (24)$$

This value agrees with the data reported by Smits et al.[27] and Dussauge et al.[14] The present value seems to be even a little above the average curve, possibly because of the larger CVA bandwidth.

IX. Some Comparisons Between CVA, CCA, and CTA

CVA, CCA, and CTA Output Spectra

At a recent meeting on test techniques, Comte-Bellot et al.[28] presented comparison of the output spectra of CVA, CCA, and CTA. The results were obtained by using the same hot wire (2.5-μm tungsten, with $2l/d \approx 200$ and $R_a \approx 5.5\ \Omega$) in the Mach 2.3 boundary layer at IRPHE, all at the same location ($y/\delta = 0.27$), at an operating overheat $a_w \approx 0.60$. The CCA was a DISA 56CO2 with a 40-dB preamplifier and a first 50-μs thermal lag correction. A special cable path for the hot-wire connection to the CCA was installed to ensure low noise. The CTA was a DISA Streamline 90C10, with a symmetric bridge and a top resistance of 20 Ω. The connecting Dantec cable was 4 m long. The same cable was used with CVA. For $a_w \approx 0.60$, the gain position was 14, the filter position 10, and the tuning -5. The representative results from these tests are shown in Fig. 13. The CTA showed a limited frequency response in this test probably from the filtering applied to the feedback loop to increase its stability. Between the CVA and CCA there is a good agreement up to 200 kHz. The spectra from the CVA showed that it had larger overall bandwidth. The CCA had a 400-kHz low-pass filter at its output. The measured bandwidth of the CVA prototype was 470 kHz, and it had a 670-kHz low-pass filter at the output. No special installation steps of any kind or any particular cable lengths were necessary for using the CVA.

CVA, CCA, and CTA Output Levels

Comparison of the output levels of the CVA, CCA, and CTA was done with the hot wire being operated at the same point (overheat and turbulence) in all of the three anemometers. From Eq. (18), the mean square value of the CVA fluctuating output is

$$\overline{e'^2_{\mathrm{CVA}}} = \left[1\big/(1+2a_w)^2\right]\left[\tfrac{1}{4}a_w^2 T^2_{\rho u} - a_w R + T^2_{\theta_t}\right]E^2_{\mathrm{CVA}} \qquad (25)$$

By the use of the following sensitivity coefficients derived by Comte-Bellot[6]:

$$S^{\mathrm{CCA}}_{\rho u} \approx -a_w/2, \qquad S^{\mathrm{CCA}}_{\theta_t} \approx 1$$
$$S^{\mathrm{CTA}}_{\rho u} \approx \tfrac{1}{4}, \qquad S^{\mathrm{CTA}}_{\theta_t} \approx -1/2a_w \qquad (26)$$

the CCA and CTA outputs would be

$$\overline{e'^2_{\mathrm{CCA}}} = \left[\tfrac{1}{4}a_w^2 T^2_{\rho u} - a_w R + T^2_{\theta_t}\right]E^2_{\mathrm{CCA}} \qquad (27)$$

$$\overline{e'^2_{\mathrm{CTA}}} = \left(1\big/4a_w^2\right)\left[\tfrac{1}{4}a_w^2 T^2_{\rho u} - a_w R + T^2_{\theta_t}\right]E^2_{\mathrm{CTA}} \qquad (28)$$

E_{CCA} is the dc voltage at the CCA output (wire plus cable). E_{CTA} is the dc voltage at the top of the CTA Wheatstone bridge. Equations (25), (27), and (28) relate the rms outputs of each anemometer to its mean output voltage. To relate the outputs in terms of the rms values irrespective of their mean values, the following equations in terms of the voltage V_w across the hot-wire are invoked. The voltage ratio E_{CVA}/V_w for the CVA is obtained by rewriting Eq. (1b) as

$$E_{\mathrm{CVA}}/V_w = R_2/[R_a(1+a_w) + r_L] + (1 + R_2/R_F) \qquad (29)$$

and similarly for the mean ratio E_{CCA}/V_w and E_{CTA}/V_w

$$E_{\mathrm{CCA}}/V_w = 1 \qquad (30)$$

$$E_{\mathrm{CTA}}/V_w = 1 + R_{\mathrm{TB}}/[R_a(1+a_w) + r_L] \qquad (31)$$

Substituting these mean voltages in the ratios obtained from Eqs. (25), (27), and (28), we obtain the following equations:

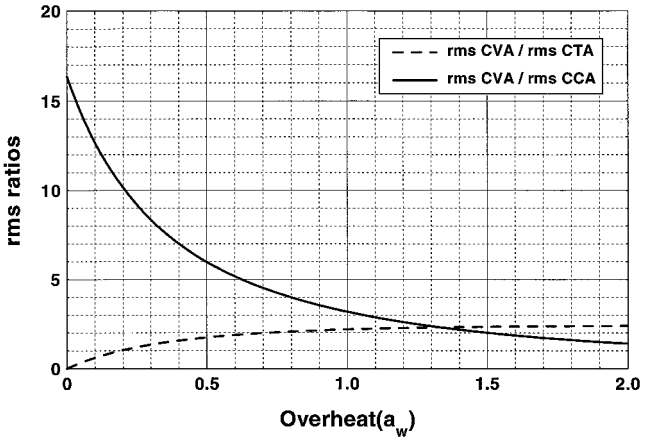

Fig. 14 Theoretically estimated ratios of rms variations of CVA with CCA and CTA.

$$\left[\frac{\overline{e'^2_{\mathrm{CVA}}}}{\overline{e'^2_{\mathrm{CCA}}}}\right]^{\frac{1}{2}} = \frac{1}{1+2a_w}\left[\frac{R_2}{R_a(1+a_w)+r_L} + \left(1+\frac{R_2}{R_F}\right)\right] \tag{32}$$

$$\left[\frac{\overline{e'^2_{\mathrm{CVA}}}}{\overline{e'^2_{\mathrm{CTA}}}}\right]^{\frac{1}{2}} = \frac{2a_w}{1+2a_w}\,\frac{R_a(1+a_w)}{R_a(1+a_w)+r_L} \times \frac{R_2/[R_a(1+a_w)+r_L]+(1+R_2/R_F)}{R_{\mathrm{TB}}/[R_a(1+a_w)+r_L]+1} \tag{33}$$

The estimated ratios from expressions (32) and (33) are plotted in Fig. 14, for $R_a \approx 5.50\ \Omega$, $r_L \approx 1.14\ \Omega$, $R_2 \approx 100\ \Omega$, $(1+R_2/R_F) \approx 1.3$ and $R_{\mathrm{TB}} = 20\ \Omega$. The overheat range a_w up to 2 was used to show the invariance at higher overheats, whereas $a_w \leq 0.80$ only was used in the experiments. Figure 14 shows that the fluctuating output voltages are definitively much higher in the CVA than in the CCA at any given operating overheat, as already suggested by Sarma.[29] Relative to the CTA, the higher sensitivity of the CVA is obtained only for $a_w \geq 0.2$. If necessary, the CVA sensitivity can be further increased with larger R_2 values at the expense of higher power dissipation in the circuit with associated marginal changes in the bandwidth. In fact, another CVA prototype uses $R_2 = 120\ \Omega$. Ratios of the square roots of the measured spectral ratios (in the most energetic parts of the spectra), CVA/CCA and CVA/CTA, are in very good agreement with the estimated values shown in Fig. 14. Note that the measured change in hot-wire resistance was 2.0% at $a_w \approx 0.17$ and 2.1% at $a_w \approx 0.50$, for the CVA, whereas that of CCA varied from 2.9 to 4.4% in the same overheat range.

X. Conclusions

Turbulence measurements with the CVA data postprocessed with in situ measured parameters was found to be accurate, simple, and highly productive. Without changing the hardware lead compensation setting during the experiment, it was possible to obtain the in situ values of the hot-wire time constant and overheat along with turbulence signals. It was also possible to acquire data at several settings of overheats from low to high values quickly without any stability problems. A very distinct advantage of such a procedure was that the CVA bandwidth remained constant for all of the tests. It was also observed from several tests that different hot-wire cable lengths did not cause any significant change in the noise levels, spectra, or stability of the CVA. Without any need for critical adjustments, cable length requirements, or optimization of its location in the test, it was found that the CVA outputs have maintained high fidelity at all of the overheats and Reynolds numbers tested. Theoretical and experimental sensitivity analysis of the CVA, CCA, and CTA indicates that the prototype CVA tested had a higher sensitivity over the other two anemometers used in the tests. It was also observed in the tests that the signal-to-noise ratio of the CVA remained larger than one even up to 450 kHz. With the reported automated features in a new CVA, it should be possible to use CVA for many applications in fluid dynamics with the advantage of having an open-loop device with highly predictable performance features.

Acknowledgments

Thanks are given to the engineers at Tao Systems who have contributed in the hardware development and testing. The authors wish to thank D. Greer [NASA Dryden Flight Research Center (DFRC)], S. M. Mangalam (Tao Systems), T. Moes (NASA DFRC) and S. P. Wilkinson (NASA Langley Research Center) for their encouragement of the constant voltage anemometer. The authors are also grateful to J. P. Dussauge, P. Dupont and J. F. Debiève for fruitful discussions and use of the IRPHE wind tunnel, and to T. M. Faure for his participation in the experiments.

References

[1]Sarma, G. R., "Flow Measuring Apparatus," U.S. Patent 5074147, 24 Dec. 1991.

[2]Sarma, G. R., and Lankes, R. W., "Automated Constant Voltage Anemometer with In-Situ Measurements of Overheat and Time Constant of the Hot-Wire," *Review of Scientific Instruments*, Vol. 70, No. 5, 1999, pp. 2384–2386.

[3]Moes, T., Sarma, G. R., and Mangalam, S. M., "Flight Demonstration of a Shock Sensor Using Constant Voltage Hot-Film Anemometry," NASA TM 4806, 1997.

[4]Lachowicz, J. T., Chokani, N., and Wilkinson, S. P., "Boundary-Layer Stability Measurements in a Hypersonic Quiet Tunnel," *AIAA Journal*, Vol. 34, No. 12, 1996, pp. 2496–2500.

[5]Lachowicz, J. T., and Chokani, N., "Hypersonic Boundary Layer Stability Experiments in a Quiet Wind Tunnel with Bluntness Effects," NASA CR-198272, 1996.

[6]Comte-Bellot, G., "Hot-Wire Anemometry," *Handbook of Fluid Dynamics*, edited by R. W. Johnson, CRC Press, Boca Raton, FL, 1998, Chap. 34.

[7]Blanchard, A. E., Lachowicz, J. T., and Wilkinson, S. P., "NASA Langley Mach 6 Quiet Wind Tunnel Performance," *AIAA Journal*, Vol. 35, No. 1, 1997, pp. 23–28.

[8]Blanchard, A. E., and Selby, G. V., "An Experimental Investigation of Wall-Cooling Effects on Hypersonic Boundary Layer Stability in a Quiet Wind Tunnel," NASA CR-198287, 1996.

[9]Kegerise, M. A., and Spina, E. F., "A Comparative Study of Constant Voltage and Constant Temperature Hot-Wire Anemometers in Supersonic Flow," 3rd International Symposium on Thermal Anemometry, July 1996.

[10]Sarma, G. R., "Transfer Function Analysis of the Constant Voltage Anemometer," *Review of Scientific Instruments*, Vol. 69, No. 6, 1998, pp. 2385–2391.

[11]Kegerise, M. A., and Spina, E. F., "Determination of the Frequency Response of a Constant Voltage Hot-Wire Anemometer," AIAA Paper 97-1915, July 1997.

[12]Kistler, A. L., "Fluctuation Measurements in a Supersonic Turbulent Boundary Layer," *Physics of Fluids*, Vol. 2, No. 3, 1959, pp. 290–296.

[13]Sarma, G. R., Comte-Bellot, G., and Faure, T. M., "Software Corrected Hot-Wire Thermal Lag for the Constant Voltage Anemometer Featuring a Constant Bandwidth at the Selected Compensation Setting," *Review of Scientific Instruments*, Vol. 69, No. 9, 1998, pp. 3223–3231.

[14]Dussauge, J. P., Smith, R. W., Smits, A. J., Fernholz, H., Finley, P. J., and Spina, E. F., "Turbulent Boundary Layers in Subsonic and Supersonic Flows," edited by W. S. Saric, AG-335, AGARD, July 1996.

[15]Corrsin, S., "Turbulence: Experimental Methods," *Handbuch der Physics/Encyclopedia of Physics*, edited by S. Flügge, Vol. 8/2, Springer, Berlin, 1963, pp. 524–590.

[16]Ko, C. L., McLaughlin, D. K., and Troutt, T. R., "Supersonic Hot-Wire Fluctuation Data Analysis with a Conduction End-Loss Correction," *Journal of Physics E: Scientific Instruments*, Vol. 11, 1978, pp. 488–494.

[17]Fingerson, L. M., and Freymuth, P., "Thermal Anemometers," *Fluid Mechanics Measurements*, edited by R. J. Goldstein, Hemisphere, New York, 1983, pp. 99–154.

[18]Morkovin, M., "Fluctuations and Hot-Wire Anemometry in Compressible Flows," AGARDograph 24, 1956.

[19]Gaviglio, J., "Sur les méthodes de l'anémométrie par fil chaud des écoulements turbulents compressibles de gaz," *Journal de Mécanique Appliquée*, Vol. 2, No. 4, 1978, pp. 449–498.

[20]Bonnet, J. P., "Etude théorique et expérimentale de la turbulence dans un sillage supersonique," Ph.D. Dissertation, No. 355, Centre d'Etudes Aérodynamiques et Thermiques, Univ. de Poitiers, Poitiers, France, June 1982.

[21]Smits, A. J., Hayakawa, K., and Muck, K. C., "Constant Temperature Hot-Wire Anemometer in Supersonic Flows, Part 1: The Normal Wire," *Experiments in Fluids*, Vol. 1, 1982, pp. 83–92.

[22]Freymuth, P., "Uber einige spezielle Probleme der Hitzdrahtmesstechnik," Deutsche Luft- und Raumfahrt, DLR Rept. FB 66-03, Berlin, Jan. 1966.

[23]Kovasznay, L. S. G., "Development of Turbulence-Measuring Equipment," NACA Rept. 1209, 1954.

[24]Dewey, C. F., Jr., "A Correlation of Convective Heat Transfer and Recovery Temperature Data for Cylinders in Compressible Flow," *International Journal of Heat and Mass Transfer*, Vol. 8, 1965, pp. 245–252.

[25]Kuppa, S., Sarma, G. R., and Mangalam, S. M., "Effect of Thermal Inertia on the Frequency Response of Constant Voltage Anemometer and its Compensation," *Fluid Measurement Instrumentation Forum*, Fluid Engineering Div., Vol. 61, American Society of Mechanical Engineers, Fairfield, NJ, 1993, pp. 67–73.

[26]Saddoughi, S. G., and Veeravalli, S. V., "Hot-Wire Anemometry Behaviour at Very High Frequencies," *Measurement Science and Technology*, Vol. 7, No. 10, 1996, pp. 1297–1300.

[27]Smits, A. J., Spina, E. F., Alving, A. E., Smith, R. W., Fernando, E. M., and Donovan, J. F., "A Comparison of the Turbulence Structure of Subsonic and Supersonic Boundary Layers," *Physics of Fluids A*, Vol. 1, No. 11, 1989, pp. 1865–1875.

[28]Comte-Bellot, G., Sarma, G. R., Faure, T., Dussauge, J. P., Dupont, P., and Debiève, J. F., "Performance Studies of the Constant Voltage Anemometer in a Mach 2.3 Boundary Layer," 18th International Congress on Instrumentation in Aerospace and Simulations Facilities, Paper 40, Toulouse, France, June 1999.

[29]Sarma, G. R., "Analysis of the Constant Voltage Anemometer Circuit," *IEEE Instrumentation and Measurement Technology Conference*, Inst. of Electrical and Electronics Engineers, New York, 1993, pp. 731–736.

R. P. Lucht
Associate Editor